IEEE Access
Multidisciplinary | Rapid Review | Open Access Journal

Received February 14, 2018, accepted March 19, 2018, date of publication March 27, 2018, date of current version April 23, 2018.

Digital Object Identifier 10.1109/ACCESS.2018.2819984

Optimal Operation Planning for Orchestrating Multiple Pulsed Loads With Transient Stability Constraints in Isolated Power Systems

FAN LI[1], YING CHEN[1], (Member, IEEE), RUI XIE[1], CHEN SHEN[1], (Senior Member, IEEE), LU ZHANG[1], (Student Member, IEEE), AND BOYU QIN[2]

[1]Department of Electrical Engineering, Tsinghua University, Beijing 100084, China
[2]State Key Laboratory of Electrical Insulation and Power Equipment, School of Electrical Engineering, Xi'an Jiaotong University, Xi'an 710049, China

Corresponding author: Chen Shen (shenchen@mail.tsinghua.edu.cn)

This work was supported in part by the National Natural Science Foundation of China under Grant 51707147, Grant 51477081, and Grant U1766206, and in part by the major basic research in the National Security of China under Grant 613294.

ABSTRACT Power systems used on shipboards, airplanes, and similar applications are usually classified as isolated power systems (IPSs), where pulsed loads are very important under both normal and extreme conditions. Because of the high energy density of pulsed loads, stable operation of an IPS with multiple types of pulsed loads faces great challenges. This paper proposes an optimal operation planning of IPS with multiple pulsed loads while considering stability constraints. To mitigate the negative effect of pulsed loads, energy storage devices are used to buffer the required energy. The stability constraints are derived from a proposed analytical criterion whose feasibility is guaranteed by fully studied principles. A critical point-based particle swarm optimization algorithm is proposed to solve the optimal planning problem. The case studies on a typical IPS with multiple pulsed loads verify the correctness and effectiveness of the proposed method.

INDEX TERMS Isolated power systems, multiple pulsed loads, transient stability constraints.

I. INTRODUCTION

A. MOTIVATION

Loads that consume a large amount of power within a very short period of time can be considered as pulsed loads [1]. Nowadays, to enhance the functionalities of vessels, various pulsed loads are integrated into an isolated power system (IPS). To improve their utility values and simultaneously maintain system stability, optimal operation planning of pulsed loads is highly required.

As introduced in [2], a pulsed load may be connected to the IPS using an energy storage device, which buffers the energy required by the pulsed load. Then, by controlling the charging and discharging of the energy storage device, the transient effects of the pulsed load can be effectively mitigated. However, if multiple pulsed loads are connected and randomly used, their cumulated power consumption could intensively vary. Consequently, IPSs with multiple pulsed loads may encounter instability issues. Thus, coordinated operation of various pulsed loads appears to be valuable for enhancing efficacy and stability of an IPS.

The main purpose of the present work is to propose an optimal operation planning to coordinate multiple pulsed loads in an IPS. Through coordinated operations, the overall utility value of the pulsed loads can be enhanced while maintaining the security of the IPS by avoiding instability issues.

B. RELATED WORKS

Energy management system is an emerging topic in the design and operation of future IPSs. Studies have mainly focused on size planning and scheduling, optimal operation, energy management, and optimized efficiency. According to the research time scale, IPSs usually operate at a very short time period, especially when special loads such as propulsion and pulsed loads are considered. As reported in [3], an energy storage system (ESS) can highly contribute to load demand management and generally to the global energy management of the IPS with possible reduction in prime movers, which in turn reduces operating cost.

However, during recent years, different attractive energy storage technologies (high power flywheels, supercapacitors,

and flow batteries) with different operating characteristics have become available [4]. In [4], the operation of a warship power system equipped with an ESS was analyzed from the economical point of view based on the Lagrange method. The energy and power balances were taken into account under the study time period of the ship power system operation to derive the system marginal cost. In [5], a hybrid ESS has been proposed to mitigate the power fluctuations of ship electric drive trains. Three different load power fluctuations were studied in [5], which significantly affected the performance and life cycle of both the involved mechanical and electrical systems. In [6], a 0.25-Hz 36-MW pulsed load was successfully used on an IPS where a dynamic reactive compensator was installed to maintain bus voltages. In [7], multiple pulsed loads with different functionalities were considered to enhance the capabilities of an IPS.

To ensure secure operations of IPSs, research studies have been conducted to survey the effect of pulsed loads as well as to develop optimal controls for them. In particular, in [8]–[13], the negative effects of pulsed loads on the stability and power quality of an IPS have been studied using transient simulations. Then, to reduce such influence, indirect integration schemes have been proposed in which pulsed loads were suggested to be connected in parallel with ESSs. In [2], [14]–[16], [19], and [20], valuable discussions were presented to address the configurations of ESSs in an IPS in terms of their power densities, transient performance, maintenance costs, and so on. We learned that supercapacitors and flywheels were popularly used in pulsed load integration [2], [17], which are generally regarded as device-level energy storage (DLES) in this study.

We suppose that pulsed loads are totally powered by the energy buffered in the DLES. Thus, to enhance the performance of the pulsed loads, advanced charging controls of the DLES are highly required. In [18], an ADP-based control method was presented based on a simplified IPS model and the ramp-rate difference of supply and demand. The algorithms were simple to implement and could effectively reduce the negative effects during supercapacitor charging. The algorithms were tested using detailed single- and multiple-generator IPS models.

Two important issues remain to be addressed. 1) The cooperation of multiple pulsed loads has not yet been investigated. 2) Analytical criteria to determine the stability of IPSs after adopting the above control strategies remain unavailable.

C. MAIN CONTRIBUTIONS

The main contributions of this study are twofold.

A coordinate strategy for multiple pulsed load-connected IPS is proposed in this paper. The stability is guaranteed by fully studied criteria.

The feasibility of the optimization has been improved by simplifying the complicated constraints. Note that we have not improved to the PSO algorithm itself. Our contribution is to simplify the constraints through concrete theory. This simplification enables the problem to be solved using traditional PSO.

The advantages of the proposed approach can be summarized as follows. First, using the proposed stability criteria, the transient stability constraints can be analytically modeled. Second, the optimal solution of the utility function considers both stability constraints and the coordination of multiple pulsed loads. Third, the critical point-based PSO algorithm can guarantee the efficiency and accuracy of the load-dispatching process with high efficiency.

D. PAPER ORGANIZATION

This paper is organized as follows. The model of the pulsed loads in an IPS is introduced in Section II. Section III proposes the optimal operation planning of multiple pulsed loads. In Section IV, the approach to maximizing the utility function of the coordinate strategy in IPS is proposed. IPSs with different types of multiple pulsed loads are considered in Section V, and time-domain simulations are performed to verify the effectiveness of the proposed method. Section VI concludes this paper.

II. MODEL OF PULSED LOADS IN IPS

A. IPS WITH MULTIPLE PULSED LOADS

Figure 1 shows a simplified topology of an IPS consisting of pulsed loads. A generator is installed, which acts as the main power source. All propulsion loads are aggregated as one load (M). Several pulsed loads are connected to the PCC bus with their respective DLESs. Moreover, a system level energy storage (SLES) is connected to the PCC bus. This SLES is responsible for smoothing the accumulated load demands of all pulsed loads and ensuring power balance of the whole IPS.

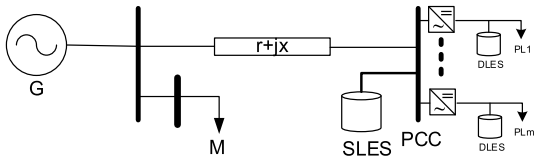

FIGURE 1. Structure of a typical IPS with pulsed loads.

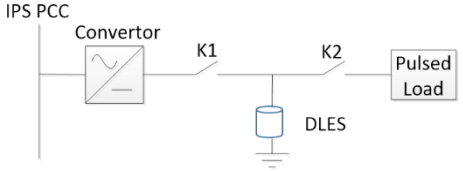

FIGURE 2. Single pulsed load connected to IPS with a DLES.

B. MODEL OF PULSED LOADS WITH DLES

We suppose that each pulsed load is connected to a PCC bus with a DLES. Figure 2 shows that the DLES is charged when K_1 is closed and K_2 is open. Then, when K_1 is open and K_2 is closed, the pulsed load is powered by the DLES to perform its function. Generally, much more time is taken for charging

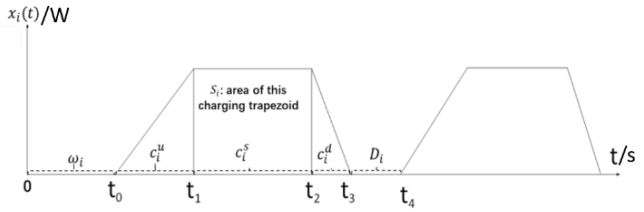

FIGURE 3. Charging power consumed by one DLES.

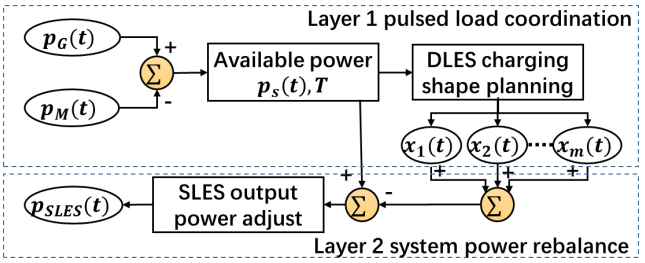

FIGURE 4. Bi-layered control structure of an IPS with pulsed loads.

the DLES than for discharging it to supply the pulsed load. Consequently, the IPS may experience relatively small load variations instead of directly energizing the pulsed load.

According to [7], the charging process of a DLES can be described by a trapezoidal shape, as shown in Fig. 3. When $t_0 \le t \le t_1$, the charging power of the DLES almost linearly increases, constrained by the ramp-up rate of the converter output power. When $t_1 \le t \le t_2$, the DLES is charged by the maximum output power of the converter. From t_2 to t_3, the charging power decreases with a certain ramp-down rate and reaches zero at t_3. During t_3 to t_4, the DLES is thoroughly discharging power to supply the pulsed load. Thereafter, it is recharged for the next round of usage. We should remember that for the DLES, the energy gained by the charging process should be equal to that released during the discharging process.

In Fig. 3, $x_i(t)$ represents the charging power consumed by the DLES while serving pulsed load i; ω_i denotes the waiting period before this pulsed load is plugged in; $c_i = c_i^u + c_i^s + c_i^d$ is the overall charging period of the DLES, where c_i^u, c_i^s, and c_i^d are the time intervals for the charging power ramping up, stable state, and ramping down, respectively; and $D_i \ge 0$ stands for a constant discharging period. The runtime cycle of the DLES is assumed to be constant as $c_i + D_i$.

We note that optimal sizing of DLES and SLES tends to be important to improve the efficiency and stability of the whole IPS and deserves to be thoroughly investigated. In this work, by focusing on optimizing the coordinated operations of the pulsed loads, we consider that the power and energy capacity of all ESSs have been previously determined.

C. BI-LAYERED CONTROL STRUCTURE OF THE IPS

As a summary, the pulsed load is indirectly connected to the IPS using buffering energy with the DLES. By adjusting the shape of the charging trapezoids of each DLES and their plug-in time, the overall power demands of the multiple pulsed loads can be regulated. Meanwhile, the SLES helps smooth this accumulated demand as well as keep the host IPS power consistently balanced. Therefore, to maximize its energy efficacy, a bi-layered control system can be developed for an IPS with multiple pulsed loads, which is shown in Fig. 4.

The first control layer is used to coordinate the operations of the pulsed loads following the variation in the available power. In other words, by carefully orchestrating the charging and discharging processes of all DLESs, the available energy over period T, can be maximally utilized by the corresponding pulsed loads. Then, in the second control layer, the output power of the SLES is dynamically adjusted to compensate the mismatches between the power supply and accumulated demand of the pulsed loads.

We can see that the first control layer enhances the utility value of the devices in the IPS, which is formulated as an optimal operation planning problem and efficiently solved in the following sections. The second control layer continuously maintains the power balance of the IPS, whose functionalities are considered in the secure and stability constraints of the proposed optimal planning model.

III. OPTIMAL OPERATION PLANNING OF MULTIPLE PULSED LOADS

A. ACTION-BASED OPTIMIZATION OBJECTIVE

We assume that a number of pulsed loads are installed in a simple IPS, as shown in Fig. 1, which are denoted as $P_{L,i}$, $i = 1, 2, \cdots, m$. For each pulsed load, a utility function is defined to measure its actions. Then, the coordinated operation should maximize the cumulative utility values of all pulsed loads during a given time interval. The objective of the optimal operation planning can be expressed as

$$max \int_0^T \sum\nolimits_{i=1}^{m} v_i(t)dt, \tag{1}$$

where $v_i(t) \ge 0$ represents the utility function of pulsed load $P_{L,i}$ and T stands for the considered time interval.

In particular, in this work, the utility value of every full action of a pulsed load is assumed to be time invariant. Thus, we obtain

$$\int_{t_0}^{t_4} v_i\,(t)\,dt = V_i, \tag{2}$$

where $V_i \ge 0$ is a constant utility value gained from the action of pulsed load $P_{L,i}$. The number of full actions of pulsed load $P_{L,i}$ is denoted by n_i, which is also a variable that needs to be optimized. Figure 3 shows that for given time interval T, n_i has an upper bound, where $\lceil\cdot\rceil$ stands for the integer operator.

$$n_i(\omega_i, c_i^u, c_i^s, c_i^d) \le \left\lceil \frac{T - \omega_i}{c_i + D_i} \right\rceil. \tag{3}$$

To understand (1)–(3) more clearly, a detailed model and real application of the DLES can be found in [7]. Thus, by adjusting waiting time ω_i and the charging intervals such as c_i^u, c_i^s, and c_i^d, the number of pulsed load actions can be flexibly regulated. By substituting (2) and (3) into (1), the objective

function of the optimal operation planning can be rewritten as

$$\max_{\omega_i, c_i^u, c_i^s, c_i^d, n_i} \sum_{i=1}^{m} V_i \cdot n_i. \tag{4}$$

Equation (4) can be seen as being aimed at optimizing the summary of the action-based utility values of all pulsed loads. Several operating constraints exist that must be considered during the coordination of the pulsed loads, which are elaborated in the next section.

B. ADEQUACY CONDITION FOR INSTANTANEOUS POWER BALANCE

The power flow balance of the IPS should be maintained while the multiple pulsed loads are working. Because all devices in the IPS are closely connected to several buses, the power flow balance of the IPS can be simplified as the instantaneous power balance constraint as follows:

$$p_G(t) + p_{SLES}(t) = \sum_{i=1}^{m} x_i(t) + p_M(t), \quad \forall t \in (0, T], \tag{5}$$

where $p_G(t)$ and $p_{SLES}(t)$ denote the output power of the generator and SLES, respectively, and $p_M(t)$ is the demand of the propulsion load.

Obviously, (5) is a time-variant constraint. It is very hard to address in optimal operation planning because all dynamics of the power sources and loads need to be thoroughly considered. To reduce the computational cost for solving the proposed planning problem, the above constraint is relaxed as an adequacy condition. This is detailed in the following.

As the concerned time interval T is relatively small, we can reasonably assume that the energy stored in the SLES will not be exhausted during the pulsed load operations. Moreover, the SLES can be quickly regulated to smooth the accumulated demands of all pulsed loads. Then, the adequacy condition of the exchange power of the SLES becomes a critical issue for the studied optimal operation planning, which can be expressed as follows:

$$\max_{0 \le t \le T} \left| \sum_{i=1}^{m} x_i(t) - p_S(t) \right| \le P_{SLES}, \tag{6}$$

where $p_s(t) = p_G(t) - p_M(t)$ stands for the available power supply to all pulsed loads and P_{SLES} is the maximum output power of the SLES. In other words, if the maximum gap between the accumulated demand and available power supply can be covered by the output power of the SLES, the instantaneous power balance of the whole IPS can always be guaranteed.

C. SHAPE CONDITION OF THE DLES CHARGING POWER

Generally, the minimum energy buffered by one DLES should be larger than the energy demand consumed by one action of the pulsed load. Such action-based energy demand can be interpreted as the area of one charging trapezoid, which is denoted as S_i in Fig. 3. Normally, the characteristics of one pulsed load remain invariant after it starts up. Thus, S_i can be regarded as a constant when pulsed load $P_{L,i}$ is operating. Then, the following condition should be satisfied for each charging of the DLES:

$$S_i = \frac{1}{2} h_i (c_i^s + c_i), \tag{7}$$

where h_i is the height of the charging trapezoid.

Meanwhile, for the DLES with pulsed load $P_{L,i}$, the ramp-up rate of the charging power is mainly constrained by the capacity of the interfacing converter. Here, this maximum ramp-up rate of the charging power is defined as λ_i^u. Similarly, during shaping of the charging power trapezoid, the constraint on power deduction of the converter should also be considered. Here, the maximum acceptable ramp-down rate is denoted as λ_i^d. Then, the following conditions should be satisfied during the charging processes of each DLES:

$$h_i \le \lambda_i^u c_i^u, \tag{8}$$

$$h_i \le \lambda_i^d c_i^d. \tag{9}$$

D. STABILITY CONDITION OF MULTIPLE PULSED LOAD OPERATION

As elaborated in [21], fast switching of large loads could cause dynamic instability issues in the IPS. In the current work, sequential operations of the pulsed loads are carefully orchestrated to keep their total demand close to the available power supply. Meanwhile, SLES is adopted to dynamically compensate the power gaps. Thus, viewed from the generator side, the overall demand of multiple pulsed loads is reshaped as a slowly changing load. Hence, the dynamic instability issues due to fast switching events are avoided.

However, while working on a ship or aircraft, the IPS may encounter large disturbance resulting from internal component failure or external effects. Thus, to ensure secure operation under such circumstances, transient voltage stability should be considered in the proposed optimal planning model.

In [22], an operator method was proposed to study the input–output stability of the power system, which rendered the stability criteria of the whole system derived from the features of its subsystems. In [23], we applied this method to analyze and enhance the transient voltage stability of a typical IPS. By evaluating the input–output gains of each subsystem, the system-level gain matrix could be formed considering flexible topology variations. Then, a small-gain condition is applied to determine the system stability according to the spectral radius of the gain matrix. By combining the offline feature evaluations of the subsystems and online stability judgment, this method shows the advantages of both flexibility and efficiency. Thus, we adopt the stability criteria proposed in [21] as a secure operating constraint of the proposed optimal planning and conduct quick stability evaluations during the search for the optimal solution. We emphasize that our method and the method in [21] are different. The approach in [21] requires both input-to-output stability and input-to-state stability of subsystems at the same time.

When a subsystem has more than one state or has nonlinear parts, the state of the subsystem is hard to determine. Our method can avoid the above problem because it only needs the input-to-output stability of the subsystems. The details of our method are given in Appendix.

Let us denote the spectral radius of the gain matrix of the studied IPS as σ. It can be written as a function as follows:

$$\sigma\left(p_G, p_M, p_L\right) = f\left(\gamma_G\left(p_G\right), \gamma_M\left(p_M\right), \gamma_L\left(p_L\right)\right), \quad (10)$$

where $\gamma_G(p_G)$, $\gamma_M(p_M)$, and $\gamma_L(p_L)$ stand for state-related input–output gains of the generator, propulsion load, and pulsed load subsystems, respectively. Further, p_L is the sum of the accumulated pulsed load demand and the output power of the SLES, that is, all pulsed loads with DLESs and the SLES composed the pulsed load subsystem. Then, following the routines given in Appendix, the subsystem gains, gain matrix, and corresponding σ can be obtained. To guarantee transient voltage stability of the IPS, the following condition should always be satisfied:

$$\sigma(p_G, p_M, p_L) < 1. \quad (11)$$

Note that if more generators and loads are used in the IPS, corresponding subsystems can be defined for them, which could be consistently considered in the secure operating constraint.

E. OVERALL OPTIMAL OPERATION PLANNING MODEL

The proposed model of the optimal operation planning of multiple pulsed loads can be summarized as follows:

$$\begin{aligned} &\text{Objective: (4)} \\ &\text{Constraints: (3), (6) , (7) , (8) , (9) , and (11).} \end{aligned} \quad (12)$$

The above model is a nonlinear programming with time-variant and non-convex constraints. In particular, in (6), the peak of the cumulated pulsed loads against $p_S(t)$ needs to be evaluated, which may involve time-costly simulations. To effectively and efficiently solve the proposed optimal operation planning model, a PSO algorithm is applied whose performance is enhanced by optimizing the initial guess of the solution and quickly determining the peaks of the total pulsed loads against $p_S(t)$.

IV. SOLUTION METHOD

A. SOLVING THE OPERATION PLANNING USING PSO ALGORITHM

The PSO algorithm [25] is adopted to solve the proposed operation planning problem. Five basic procedures are involved in the solution, which are listed as follows.

1) A set of operation configurations and variations, which are recorded as $\{z\}$ and $\{\upsilon\}$, respectively, is randomly initialized. Each z is coded by the action time variables of all pulsed loads, such as $z = \left\{\omega_i, c_i^u, c_i^s, c_i^d\right\}, i = 1, 2, \cdots m$. Meanwhile, every v represents a combination of variations of all action times planned, that is, $v = \left\{\Delta\omega_i, \Delta c_i^u, \Delta c_i^s, \Delta c_i^d\right\}$.

2) We check the satisfaction of constraints (3), (7), (8), (9), and (11). If the constraints are not satisfied, procedure 1) is repeated to perform re-initialization. Otherwise, all feasible operation configurations are marked as candidate solutions, which are denoted as $\{q\}$.

3) If the maximum number of search iterations is reached, procedure 5) is performed. Each candidate solution is updated using a random choice of v.

4) We check whether the newly generated operation configuration satisfies all constraints. If not, we ignore such a new configuration. Otherwise, we include this new configuration into the candidate solution set and return to procedure 4).

5) We select the optimal solution from the candidate solution set.

B. DEALING WITH DIFFICULTIES CAUSED BY CONSTRAINT (6)

Obviously, among all the concerned constraints, constraint (6), which is time-variant and non-convex, is the most complicated one. It imposes two difficulties on the PSO-based solution method. First, generating a new feasible operation configuration is difficult when (6) is considered. Because the capacity of the SLES is limited, $\sum x_i(t)$ should always closely track $p_S(t)$ during period T. Thus, the feasible solution space is intensively squeezed due to (6), which makes procedure 4) seldom find new feasible configurations, and the whole algorithm fails. Moreover, the maximum power gap between the available power supply and accumulated power demand of the pulsed loads needs to be evaluated, which tends to be time consuming.

To prevent failure in generating new feasible solutions, a penalty function is used, instead of directly considering constraint (6). The penalty method is defined as follows:

$$\sigma = -\left(max\left(\Delta P, 0\right)\right)^2, \quad (13)$$

where $\Delta P = \max\limits_{0\le t\le T}\left|\sum_{i=1}^{m} x_i(t) - p_S(t)\right| - P_{SLES}$. Then, the objective function of the optimal operation planning problem is rewritten as (4) + (13). After this transformation, the optimal operation planning problem becomes easy to solve using the PSO algorithm. When the optimal solution is obtained with $\sigma = 0$, constraint (6) will be satisfied.

Furthermore, to efficiently evaluate the maximum power gap, a critical point point-based method is proposed here. Note that $\sum_{i=1}^{m} x_i(t)$ can be regarded as a piecewise linear function because it is composed of piecewise linear charging curves. Meanwhile, when the fast-changing dynamics is ignored, available power supply $p_s(t)$ can also be approximated by a piecewise linear function. Therefore, $\sum_{i=1}^{m} x_i(t) - p_S(t)$ is a piecewise linear curve whose maximum and minimum values occur only at non-differentiable points. In other words, when either $\sum_{i=1}^{m} x_i(t)$ or $p_S(t)$ is not differentiable because their left and right derivatives are not equal, an extreme power gap may occur. Consequently, constraint (6) holds for all $t \in (0, T]$, if and only if it holds at all non-differentiable points of $x_i(t)$, $1 \le i \le m$ and $p_S(t)$.

For $x_i(t)$, the set of non-differentiable points can be represented as follows:

$$A_i = \left\{ t = \left\{ \begin{array}{c} \omega_i + (c_i + D_i)\, k \\ \omega_i + c_i^u + (c_i + D_i)\, k \\ \omega_i + c_i^u + c_i^s + (c_i + D_i)\, k \\ \omega_i + c_i^u + c_i^s + c_i^d + (c_i + D_i)\, k \end{array} \right\} \right. \left. \begin{array}{c} \\ \\ \\ \\ 0 \le t \le T, k = 0, 1, 2, \cdots \end{array} \right\}. \quad (14)$$

We assume that $p_s(t), 0 \le t \le T$ is a piecewise linear function determined by interpolation points $(t_0, p_s(t_0)), (t_1, p_s(t_1)), \cdots, (t_N, p_s(t_N))$. Then, the set of non-differentiable points of $p_s(t)$ can be expressed as follows:

$$A_s = \{t_0, t_1, \cdots, t_N\}. \quad (15)$$

Hence, the maximum power gap during the whole period can be accurately evaluated by comparing the power gaps at these time moments in $\left(\bigcup_{i=1}^{m} A_i\right) \cup A_s \cup \{0, T\}$. Because the number of considered time moments is limited, the above-mentioned evaluation tends to be very efficient.

V. CASE STUDY

A. CONFIGURATION OF THE TEST SYSTEM

An IPS with the topology shown in Fig. 1 is considered as the test system. We assume that the maximum output power of the generator is 15 MW, and the demand of the propulsion load changes following a given trajectory. The time interval for operation planning of multiple pulsed loads is set as 600 s. During this period, the host vessel is required to speed up and maximize utilization of the installed pulsed loads. The trajectories of $p_G(t)$, $p_M(t)$, and $p_S(t)$ are shown in Fig. 5, where the ramp-up and ramp-down rates of the power generation are almost fixed.

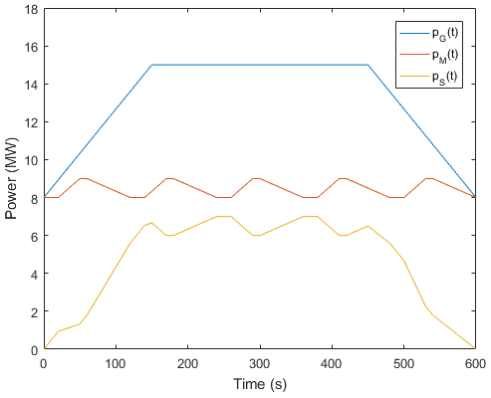

FIGURE 5. Variations in generator, propulsion load and sources.

Eight pulsed loads are integrated into the test system, whose parameters are listed in Table 1. To verify the proposed optimal planning method, the parameters of these pulsed loads are configured as totally different from one another. In particular, maximum ramp-up rate λ_i^u of the charging power is set to 400 kW/s for each pulsed load, whereas maximum acceptable ramp-down rate λ_i^d is set to 800 kW/s.

TABLE 1. Parameters of the pulsed loads.

No.	S (MJ)	D (s)	V (PA)	No.	S (MJ)	D (s)	V (PA)
1	80	5	10	5	145	8	16
2	160	7	25	6	130	9	20
3	120	10	18	7	90	6.5	8
4	105	6	13	8	110	11	19

* PA means utility value assigned for per action of a pulsed load

TABLE 2. Optimal optimization planning result.

No.	ω (s)	c^u (s)	c^s (s)	c^d (s)	n
1	134.6	158.5	28.1	76.7	1
2	145.9	41.3	16.2	70.9	3
3	51.0	73.2	28.7	23.3	4
4	54.4	39.4	52.4	20.4	4
5	128.6	43.4	35.9	55.5	3
6	18.0	23.2	52.7	38.7	4
7	28.5	23.0	11.1	74.6	4
8	76.2	47.7	14.7	57.5	4

For the PSO algorithm, the population size is fixed at 1000, whereas the maximum number of iterations is set to 3000. Other parameters related to constraint (11) are provided in Appendix, where the corresponding evaluation method is also given.

B. TEST RESULTS OF THE BASE CASE

We assume that $P_{SLES} = 2$ MW. Then, using the above-mentioned parameters, the proposed operation planning can be solved, and the results are listed in Table 2. Note that the charging time of the DLES depends on the load size, which is determined by the selection of the test parameters. The effectiveness and correctness of the method we proposed remain unchanged.

Figure 6 shows the dynamics of the charging power of each pulsed load as well as their cumulative power. We can see that $\sum x_i(t)$ continuously charges during the planning period. It closely tracks available power $p_S(t)$ while remaining in the feasible operating state space. In addition, Fig. 6 shows that the feasible operating state space for $\sum x_i(t)$ is outlined by the green dashed lines, which is mainly determined by constraints (6) and (11). Figure 6 also shows the dynamics of $x_i(t)$. By properly shaping the charging power, the orchestration of all pulsed loads becomes controllable.

C. EFFICACY OF THE PROPOSED METHOD UNDER DIFFERENT SCENARIOS

1) RESULTS OF THE SCENARIOS WITH VARIED $p_S(t)$

We suppose that the shape of $p_S(t)$ can be proportionally varied from its original value shown in Fig. 5. Then, for each level of $p_S(t)$, the optimal operation planning can be solved; the results are listed in Table 3.

We can see that when $p_S(t)$ generally increases, the objective function value of the optimal operation planning also

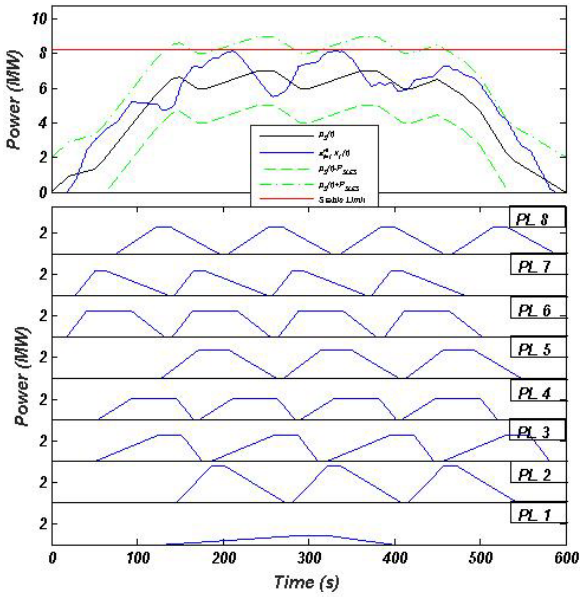

FIGURE 6. Dispatching of pulsed loads.

TABLE 3. Results of the scenarios with varied $p_S(t)$.

$p_S(t)$	Objective function value	$\sum_{i=1}^{m} n_i$
50%	294	17
75%	402	24
100%	445	27
125%	490	31
150%	Not converged	
200%	Not converged	

increases. Such a result is reasonable because more energy is supplied to the pulsed loads, which can be operated for more actions. However, as $p_S(t)$ becomes too large, no feasible solution can be obtained at all because P_{SLES} remains the same, which makes the lower bound of $\sum_{i=1}^{m} x_i(t)$ also become large. Restricted by the maximum ramp-up and ramp-down rates of the charging power, the orchestration of the pulsed loads cannot become sufficiently large to reach such a lower bound.

2) RESULTS OF SCENARIOS WITH VARIED P_{SLES}

We let the other conditions be the same while only proportionally changing P_{SLES} . Then, the optimal operation planning results can be solved, as listed in Table 4.

From Table 4, we can be see that when P_{SLES} increases, better optimal planning results are obtained. Actually, P_{SLES} is a critical factor for dynamically maintaining the power balance in the proposed control structure. If the capacity of the SLES is large, the feasible operating state space of the pulsed loads can be remarkably expanded. Then, better planning results can be searched for by the PSO method. In contrast, when P_{SLES} is 0.5 MW, no feasible solution can be found, which indicates the inadequacy of the SLES.

TABLE 4. Results of scenarios with varied P_{SLES}.

P_{SLES} (MW)	Objective function value	$\sum_{i=1}^{m} n_i$
0.5	Not converged	
1	415	24
2	445	27
4	487	25

TABLE 5. Result by varying the concerned time interval.

T (s)	Objective function value	$\sum_{i=1}^{m} n_i$	Runtime (s)
300	222	13	105
600	445	27	125
900	618	42	152
1200	783	52	178

TABLE 6. Result by varying the number of pulsed loads.

m	Objective function value	$\sum_{i=1}^{m} n_i$	Runtime (s)
2	Not converged		
4	399	24	728
6	440	26	234
8	445	27	125

3) RESULTS OF SCENARIOS WITH VARIED T

We suppose that planning period T is proportionally varied while $p_S(t)$ is accordingly scaled up or down in the time horizon. Then, the operation planning results are solved and listed in Table 5.

As T increases, the optimal planning renders better utility value of the pulsed loads. The number of actions of the pulsed loads also consistently increases. Meanwhile, the time cost for solving the proposed optimal planning problem slowly increases, which partially proves the efficiency of the proposed solution method.

4) RESULTS OF SCENARIOS WITH VARIED m

We change the number of pulsed loads m by reserving the first m pulsed loads of the eight ones in Table 2 while the other conditions remain the same. Then, the operation planning results are solved and listed in Table 6.

As m decreases, the objective function value decreases because fewer pulsed loads can be planned and the feasible region becomes smaller. The runtime consistently increases because of the PSO algorithm adopted in this study. When m is smaller, the randomly generated operation configuration more probably satisfies constraints (3), (7), (8), and (9). Thus, in each iteration, more operation configurations need to be checked for the objective function value, constraint (6), and constraint (11); however, this process takes up a major portion of the calculation. When m is too small, the total

charging power curve fluctuates too much for a feasible solution.

VI. SUMMARY OF CONTRIBUTIONS

This paper has presented a novel idea on the optimal dispatch of pulsed loads in IPS whose major advantage is its ability to guarantee not only stability but also optimality of the IPS. According to the operator approach, an analytical stability criterion is established and acts as a stability constraint in the optimization problem. Multiple types of pulsed loads are considered as a combination of cycle trapezoid curves whose maximum value is discussed and guaranteed by the proposed theorem with a rigorous proof. A PSO algorithm is proposed to ensure the efficiency and accuracy of the problem-solving process. Applications to an IPS consisting of generators, energy storage devices, and pulsed loads are presented. The effectiveness of the proposed optimal dispatch strategy is verified by time-domain simulations.

APPENDIX
SUBSYSTEM GAINS, GAIN MATRIX, AND CORRESPONDING σ

For the ith subsystem, mapping h_i can be divided into linear and nonlinear parts, as discussed in [24]. The linear part can be represented by an operator norm denoted by $\|L_i\|$, and the nonlinear part can be denoted by conic gain $\{C_i, R_i\}$, as shown in Fig. 7.

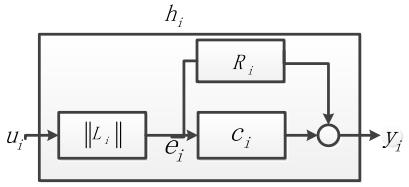

FIGURE 7. Input–output relationship of the ith subsystem.

Knowing that an unknown stable system can be factorized into a series combination of stable linear and nonlinear parts, we can proceed to independently identify them.

Through time-domain simulation, random disturbances are injected to identify the input–output properties of each subsystem. Injecting a small-signal perturbation around the steady-state operating point would nullify the nonlinear effects and would be appropriate for identifying the linear part. Meanwhile, the nonlinear part can be identified under large-signal perturbations. Here, $\|\boldsymbol{L_G}\|$ and (C_G, R_G) denote the linear and nonlinear parts of the generator, respectively. With regard to the loads (propulsion and pulsed loads), the input (random disturbance) is chosen as a voltage, whereas the output is chosen as a current. Moreover, $\|\boldsymbol{L_M}\|$ and (C_M, R_M) denote the linear and nonlinear parts of the propulsion load, whereas $\|\boldsymbol{L_L}\|$ and (C_L, R_L) denote the linear and nonlinear parts of the pulsed load.

According to the small-gain theorem, constraints $\sigma(p_G, p_M, p_L) < 1$ can be rewritten as follows:

$$\sigma\left(p_G, p_M, p_L\right) = \rho\left(\boldsymbol{NLZ}\right), \tag{16}$$

where $\boldsymbol{L}$ consists of each subsystem gain function of the linear parts:

$$\boldsymbol{L} = \begin{bmatrix} \|\boldsymbol{L_G}\| & & \\ & \|\boldsymbol{L_M}\| & \\ & & \|\boldsymbol{L_L}\| \end{bmatrix}, \tag{17}$$

$\boldsymbol{N}$ consists of each subsystem nonlinear gain:

$$\boldsymbol{N} = \begin{bmatrix} C_G + R_G & & \\ & C_M + R_M & \\ & & C_L + R_L \end{bmatrix}, \tag{18}$$

and $\boldsymbol{Z} = (z_{ij})_{i,j=1}^{n}$ denotes the input–output interconnection matrix of the subsystems.

When the above-described evaluation method is used in the particular case in Section V, the parameters are chosen as follows: $\|\boldsymbol{L_G}\| = 0.95$, $\|\boldsymbol{L_M}\| = 0.97$, $\|\boldsymbol{L_L}\| = 0.92$, $(C_G, R_G) = (1.03, 1.42)$, $(C_M, R_M) = (1.01, 1.35)$, $(C_L, R_L) = (1.02, 1.51)$, $r = 0.5$, and $X = 0.32$.

REFERENCES

[1] X. Feng, K. L. Butler-Purry, and T. Zourntos, "A multi-agent system framework for real-time electric load management in MVAC all-electric ship power systems," *IEEE Trans. Power Syst.*, vol. 30, no. 3, pp. 1327–1336, May 2014.
[2] P. F. Ribeiro, B. K. Johnson, M. L. Crow, A. Arsoy, and Y. Liu, "Energy storage systems for advanced power applications," *Proc. IEEE*, vol. 89, no. 12, pp. 1744–1756, Dec. 2001.
[3] A. Anvari-Moghaddam, T. Dragicevic, J. C. Vasquez, and J. M. Guerrero, "Optimal utilization of microgrids supplemented with battery energy storage systems in grid support applications," in *Proc. 1st IEEE Int. Conf. DC Microgrids*, Atlanta, GA, USA, Jun. 2015, pp. 57–61.
[4] K. K. Tafanidis, K. D. Taxeidis, G. J. Tsekouras, and F. D. Kanellos, "Optimal operation of war-ship electric power system equipped with energy storage system," *J. Comput. Model.*, vol. 3, no. 4, pp. 41–60, 2013.
[5] J. Hou, J. Sun, and H. F. Hofmann, "Mitigating power fluctuations in electric ship propulsion with hybrid energy storage system: Design and analysis," *IEEE J. Ocean. Eng.*, vol. 43, no. 1, pp. 93–107, Jan. 2018, doi: 10.1109/JOE.2017.2674878.
[6] M. Falahi, K. L. Butler-Purry, and M. Ehsani, "Reactive power coordination of shipboard power systems in presence of pulsed loads," *IEEE Trans. Power Syst.*, vol. 28, no. 4, pp. 3675–3682, Nov. 2013.
[7] M. Ibrahim, S. Jemei, G. Wimmer, and D. Hissel, "Nonlinear autoregressive neural network in an energy management strategy for battery/ultra-capacitor hybrid electrical vehicles," *Electr. Power Syst. Res.*, vol. 136, pp. 262–269, Jul. 2016.
[8] V. Salehi, B. Mirafzal, and O. Mohammed, "Pulse-load effects on ship power system stability," in *Proc. 36th Annu. Conf. IEEE Ind. Electron. Soc.*, Nov. 2010, pp. 3353–3358.
[9] M. Steurer *et al.*, "Investigating the impact of pulsed power charging demands on shipboard power quality," in *Proc. IEEE Elect. Ship Technol. Symp.*, May 2007, pp. 315–321.
[10] L. N. Domaschk, A. Ouroua, R. E. Hebner, O. E. Bowlin, and W. B. Colson, "Coordination of large pulsed loads on future electric ships," *IEEE Trans. Magn.*, vol. 43, no. 1, pp. 450–455, Jan. 2007.
[11] F. Sculler, "Simulation of an energy storage system to compensate pulsed loads on shipboard electric power system," in *Proc. IEEE Electr. Ship Technol. Symp.*, Apr. 2011, pp. 396–401.
[12] F. Sculler, "Study of a supercapacitor energy storage system designed to reduce frequency modulation on shipboard electric power system," in *Proc. 38th Annu. Conf. IEEE Ind. Electron. Soc. (IECON)*, Oct. 2012, pp. 4054–4059.
[13] A. T. Elsayed and O. A. Mohammed, "Distributed flywheel energy storage systems for mitigating the effects of pulsed loads," in *Proc. PES Gen. Meeting Conf. Expo.*, Jul. 2014, pp. 1–5.
[14] S. Kulkarni and S. Santoso, "Impact of pulse loads on electric ship power system: With and without flywheel energy storage systems," in *Proc. IEEE Electr. Ship Technol. Symp.*, Apr. 2009, pp. 568–573.

[15] B. Vural and C. S. Edrington, "A novel inductive-capacitive pulse forming circuit for pulse power load applications," in *Proc. 38th Annu. Conf. IEEE Ind. Electron. Soc. (IECON)*, Oct. 2012, pp. 4446–4450.
[16] J. Mcgroarty, J. Schmeller, R. Hockney, and M. Polimeno, "Flywheel energy storage system for electric start and an all-electric ship," in *Proc. IEEE Electr. Ship Technol. Symp.*, Jul. 2005, pp. 400–406.
[17] A. Mohamed, V. Salehi, and O. Mohammed, "Real-time energy management algorithm for mitigation of pulse loads in hybrid microgrids," *IEEE Trans. Smart Grid*, vol. 3, no. 4, pp. 1911–1922, Dec. 2012.
[18] L. Tan, Q. Yang, W. Im, and W. Liu, "Adaptive critic design based cooperative control for pulsed power loads accommodation in shipboard power system," *IET Generat., Transmiss. Distrib.*, vol. 10, no. 11, pp. 2739–2747, 2016.
[19] W.-S. Im, C. Wang, L. Tan, W. Liu, and L. Liu, "Cooperative controls for pulsed power load accommodation in a shipboard power system," *IEEE Trans. Power Syst.*, vol. 31, no. 6, pp. 5181–5189, Nov. 2016.
[20] C. R. Lashway, A. T. Elsayed, and O. A. Mohammed, "Hybrid energy storage management in ship power systems with multiple pulsed loads," *Electr. Power Syst. Res.*, vol. 141, pp. 50–62, Dec. 2016.
[21] B. Qin, X. Zhang, J. Ma, S. Mei, and D. J. Hill, "Local input to state stability based stability criterion with applications to isolated power systems," *IEEE Trans. Power Syst.*, vol. 31, no. 6, pp. 5094–5105, Nov. 2016.
[22] M. Barenthin, B. Wahlberg, H. Hjalmarsson, and M. Barkhagen, "Data-driven methods for L_2-gain estimation," *IFAC Proc. Volumes*, vol. 42, no. 10, pp. 1597–1602, 2009.
[23] F. Li, Y. Chen, B. Qin, and C. Shen, "Decomposed input-output stability analysis and enhancement of integrated power systems," *Sci. China Technol. Sci.*, vol. 61, no. 3, pp. 427–437, 2017.
[24] H. Phuong, "Stability analysis of large-scale power electronics systems," Ph.D. dissertation, Dept. Elect. Eng., Virginia Polytech. Inst. State Univ., Virginia Tech, Blacksburg, VA, USA, 1994, pp. 3–174.
[25] J. Kennedy and R. Eberhart, "Particle swarm optimization," in *Proc. IEEE Int. Conf. Neural Netw. (ICNN)*, Nov./Dec. 1995, pp. 1942–1948.

FAN LI received the B.E. degree in electrical engineering from Tsinghua University, Beijing, China, in 2011, where he is currently pursuing the Ph.D. degree with the Department of Electrical Engineering and Applied Electronic Technology. His research interests include transient stability analyses, isolated power systems, and pulsed load energy management.

YING CHEN (M'07) received the B.E. and Ph.D. degrees in electrical engineering from Tsinghua University, Beijing, China, in 2001 and 2006, respectively. He is currently an Associate Professor with the Department of Electrical Engineering and Applied Electronic Technology, Tsinghua University. His research interests include parallel and distributed computing, electromagnetic transient simulation, cyber-physical system modeling, and cyber security of smart grid.

RUI XIE received the B.E. degree in electrical engineering from Tsinghua University, Beijing, China, in 2017, where she is currently pursuing the Ph.D. degree in electrical engineering. Her research interests include the planning of power systems and energy storage systems.

CHEN SHEN (M'98–SM'07) received the B.E. and Ph.D. degrees in electrical engineering from Tsinghua University, Beijing, China, in 1993 and 1998, respectively. From 1998 to 2001, he held a post-doctoral position at the Department of Electrical Engineering and Computer Science, Missouri University of Science and Technology, MO, USA. From 2001 to 2002, he was a Senior Application Developer with ISO New England Inc., MA, USA. He has been a Professor with the Department of Electrical Engineering, Tsinghua University, since 2009, where he is currently the Director of the Research Center of Cloud Simulation and Intelligent Decision-Making, Energy Internet Research Institute. He is an author/co-author of over 150 technical papers and one book, and holds 21 issued patents. His research interests include power system analysis and control, renewable energy generation, and smart grids.

LU ZHANG (S'13) was born in Beijing, China, in 1990. He received the B.S. degree in electrical engineering and the Ph.D. degree in agricultural electrification and automation from China Agricultural University, Beijing, China, in 2011 and 2016, respectively. He currently holds a post-doctoral position at Tsinghua University. His main research interests include hybrid ac/dc distribution networks, renewable energy generation, and active distribution networks.

BOYU QIN received the B.S. degree in electrical engineering from Xi'an Jiaotong University, Xi'an, China, the Ph.D. degree in electrical engineering from Tsinghua University, Beijing, China, in 2011 and 2016 respectively. He is currently a Lecturer with the School of Electrical Engineering, Xi'an Jiaotong University. His research interests include power system stability analysis and control, and input-to-state stability theory.